Trans. of the Society of Instrument and Control Engineers
Vol.E-1, No.1, 197/204 (2001)

Angular Acceleration Sensor Composed of Two Discs and Optical Pick-Up†

— Analysis of Basic Performances —

Ivan Godler*, Akira Akahane**,
Toshiki Maruyama** and Tadashi Yamashita***

Acceleration is frequently used in motion control. It is usually obtained as a time derivative of position, which is measured by an encoder. A time derivative is corrupted by high frequency noise and is not reliable at low rotational speed. Since there is no appropriate angular acceleration sensor available at present, we propose a new type of angular acceleration sensor which has unlimited rotational sensing range and sufficient sensitivity to be used in motion control. The proposed sensor is composed of two discs. One of them is a spring-inertia acceleration transducer and the other is a disc similar to the discs of pulse encoders. A pair of optical pick-ups is used to measure a relative angular displacement between the two discs. In this way non-contact and speed independent angular acceleration sensing is realized. Some basic performances of the sensor are discussed in this paper: it is shown that linearity of the sensor can be improved by slits with a shape of Archimedes' spiral; eccentricities of the shaft and the discs are analyzed and a sufficient but not ideal compensation is provided by two optical pick-ups that are placed diametrically on the opposite sides of the discs. Experimental results show that the sensor's output excellently matches with the calculated acceleration.

Key Words: sensor, angular acceleration, slit disc, optical pick-up, motion control

1. Introduction

To build a control system with good performances it is important to provide a reliable and exact sensing. Rotary pulse encoders are widely used as motion sensors because of their reliability and accuracy. Encoders with high resolution can be produced, so that position sensing with satisfactory accuracy is available. However, pulse encoders have some disadvantages which are related to their incremental type of the output. Specially when the speed or acceleration is to be derived from the output of an encoder, high frequency noise is generated. This is particularly critical when the rotational speed is slow.

Methods to reduce the noise generation have been proposed. At low rotational speed, when pulses from an encoder are not available in each sampling instant, an observer is used to estimate the speed [1]. Both modeled inertia and applied torque are used to estimate acceleration, from which the speed is calculated. From the calculated speed the position is derived by integration. The calculated speed is then corrected by referring to the difference of the calculated and the sensed position. This can be performed only in the sampling instants when pulses from an encoder are available. Accuracy of the so obtained speed is strongly dependent on the exactness of estimated inertia. To improve performance of the method, an on-line estimation of the inertia was proposed [2]. The method requires considerable amount of computational time, and is sensitive to noise.

Additionally, recently developed control strategies often use acceleration or even its derivative in purpose to improve robustness of the control system. In these cases the acceleration is obtained as a time derivative of position. When a pulse encoder is used as a position sensor, high frequency noise is generated when the acceleration is calculated [3]. To reduce the noise, a low-pass filter is used. Both the noise and the lag of a low-pass filter reduce robustness of the controller. Tuning the cut-off frequency of the filter is a trade-off between the noise level and the phase lag of the filter.

The above two examples of unsatisfactory performances of calculation of speed and acceleration from a pulse encoder output suggest that both poor characteristics at low speed and robustness of the control system can be improved by directly sensed acceleration. An induction type

† Presented 32nd SICE Annual Conference (1993·8)
* University of Kitakyushu, 1–1 Hibikino, Wakamatsu-ku, Kitakyushu, Japan
** Harmonic Drive Systems, Inc., 1856–1 Oaza-Maki, Hotaka-machi, Minamiazumi-gun, Nagano, Japan
*** Kyushu Institute of Technology, 1–1 Sensui, Tobata-ku, Kitakyushu, Fukuoka, Japan

angular acceleration sensor was proposed [4]. It has disadvantages of low sensitivity and generation of harmonic noise. Since at present there is no appropriate angular acceleration sensor available, linear acceleration pick-ups which are mounted at radial distance from the rotation center are used instead. Development of an angular acceleration sensor by using silicon beams was reported [5]. This sensor has a disadvantage which is common to all linear acceleration pick-ups used as an angular acceleration sensor; that is a need for a physical connection of the rotating pick-ups and the standstill environment. Available rotational range of the device is limited to few turns, and so it can be used only in specific applications.

With an aim to develop a sensor that can be widely used in the applications where angular acceleration is needed, we propose a new type of angular acceleration sensor [6), 7]. It is composed of two discs and optical pick-ups which enable non-contact and speed independent sensing of angular acceleration.

A structure of the proposed sensor is presented in the paper and some basic performances of the device are discussed. Equations for sensitivity are derived. Analysis of linearity shows that it can be improved by the slits which are shaped into segments of an Archimedes' spiral. An error, which is caused by the eccentricity of the shaft and the discs' assembly, is evaluated, too. It is confirmed that the eccentricity error is sufficiently compensated by two identical pick-ups on diametrically opposite sides of the discs. Finally, a result of experiment with a prototype device is presented. A good agreement of the calculated and the sensed acceleration is confirmed. The error, which is caused by mechanical inaccuracies of the prototype, is to be reduced in the future designs.

2. Structure of Proposed Sensor

A principle of acceleration sensing by the proposed sensor is outlined in **Fig. 1**. The sensor itself is composed of three subsystems: mechanical, optical and electrical. Each of them has the following functions:

Mechanical part transforms angular acceleration into a displacement by a mechanical spring-inertia transducer.

Optical part transforms the displacement into an electrical signal by optical pick-ups.

Electrical part has a task to condition the signals from the optical pick-ups in such a manner that the final output of the sensor is proportional to the applied acceleration.

2. 1 Mechanical Structure

A mechanical part of the sensor is composed of two discs which are mounted on the same shaft. One of the discs is similar to the disc of a pulse encoder, while the other disc is a mechanical transducer. Both discs are shown in **Fig. 2**.

The mechanical transducer, a so called flexible disc, is composed of two rings, an inner ring and an outer ring, and of a few flexible bars which connect the two rings. The inner ring is fixed to a shaft of the sensor, while the outer ring is movable relative to the inner ring due to flexibility of the bars. Stiffness of the flexible bars and inertia of the outer ring form a second order mechanical transducer, which transforms the acceleration into a displacement. When the angular acceleration is applied to the shaft of the sensor, the outer ring is angularly displaced relative to the inner ring. In this way the acceleration is transformed into a relative angular displacement of the outer ring against the inner ring. A basic dynamic equation of the mechanical transducer is

$$J\ddot{\theta} + k\phi = 0\,. \tag{1}$$

Here J is inertia of the outer ring, $\ddot{\theta}$ is applied angular acceleration, k is stiffness of the flexible bars, and ϕ is the relative angular displacement of the outer ring against the inner ring. Damping of the disc is low and is neglected.

2. 2 Optical Pick-Up

To transform the output of mechanical transducer into

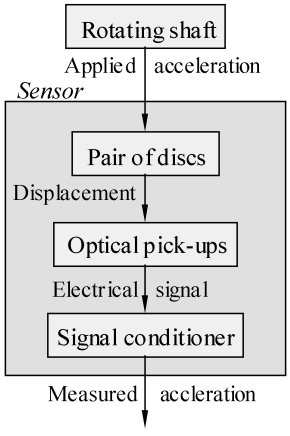

Fig. 1 Principle of acceleration sensing

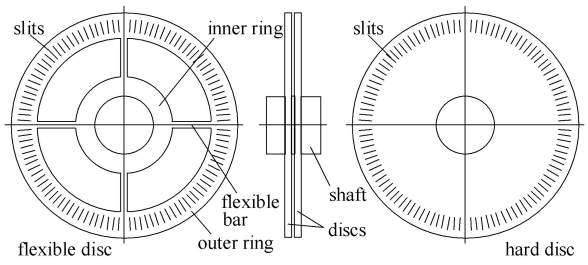

Fig. 2 Structure of mechanical parts

an electrical signal, it is necessary to measure the relative displacement of the rings. Direct sensing of the relative displacement between the outer ring and the inner ring is difficult to be realized. We use an equivalent solution, that is, sensing of a relative displacement of the outer ring against the other disc (hard disc) instead. For this purpose the slits are cut on peripheries of both discs. This enables non-contact optical sensing of the angular acceleration. A section of the slits expanded into circular direction is shown in **Fig. 3**.

Slits on one of the discs are cut in a radial direction, while the slits on the other disc are inclined for a small angle against the radial ones. A relative angular displacement of the slits (horizontal in Fig. 3) is transformed into a radial displacement of the slits crossing sections (vertical in Fig. 3). An optical pick-up, which is composed of a light emitting diode (LED) and a one dimensional position sensitive device (PSD), is used to sense the radial displacement. LED and PSD are placed on opposite sides of the discs, facing each other (see **Fig. 4**). The emitted light from LED passes the slits crossing sections and falls onto a sensitive area of the PSD, which is oriented so that a radial position of the passing light beam is detected. Two identical optical pick-ups are placed apart at 180° angular positions to compensate the error, which is caused by eccentricity of the shaft center relative to the rotation center.

2. 3 Signal Conditioning

PSD is a semiconductor device with a photo-sensitive layer. Output of a one-dimensional device is composed of two electrical currents i_A and i_B from the two terminals on both edges of a sensitive area with length L (refer to **Fig. 5**). Strength of both currents is proportional to a position of the center of the beam and to its power [8]. A relative position of the beam P is obtained by eq. (2).

$$P = \frac{i_A - i_B}{i_A + i_B} L \tag{2}$$

To avoid division, which is not accurate for small signals, we applied control of the LED output power as it is indicated in Fig. 5. The sum of the PSD outputs is held constant by closed loop control of the LED output power. By this principle a constant denominator of eq. (2) is assured, so that the position of the light beam is proportional to the difference of the PSD's outputs i_A and i_B.

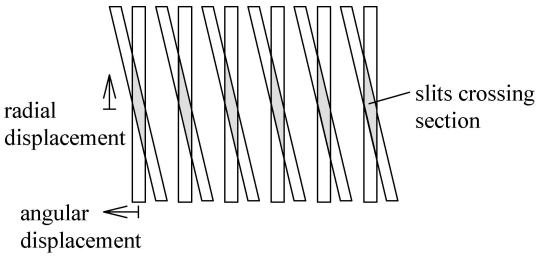

Fig. 3 Pattern of straight slits on both discs

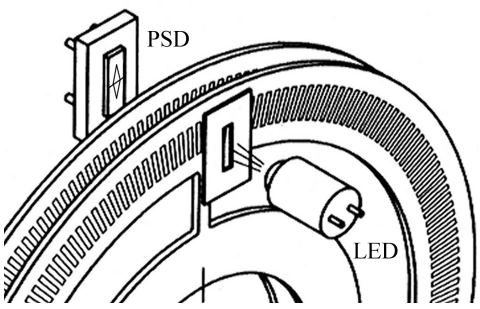

Fig. 4 Position of optical pick-ups

3. Sensitivity

In this section we discuss about sensitivity of the sensor and show, that the total sensitivity of the sensor can be separated into two partial sensitivities: mechanical sensitivity and optical sensitivity. By maximizing both of them the highest total sensitivity of the sensor is achieved.

3. 1 Mechanical Sensitivity

Mechanical sensitivity S_M is defined as a ratio of the angular displacement of the slits ϕ to the applied acceleration $\ddot{\theta}$ in the steady state. Introducing eq. (1) into the definition gives an equation for mechanical sensitivity.

$$S_M = \left| \frac{\phi}{\ddot{\theta}} \right| = \frac{J}{k} = \frac{1}{\omega_n^2} \tag{3}$$

Here ω_n is a natural frequency of the flexible disc. Note that the mechanical sensitivity is inversely proportional to the square of a natural frequency of the sensor. This relation tells that the sensitivity of the sensor is high at low natural frequency. This is in contradiction to the desire to have a sensor with wide frequency band. Therefore, the highest mechanical sensitivity is provided by the lowest possible natural frequency which still satisfies the required frequency characteristics.

Equations for inertia of the outer ring and for stiffness of the flexible bars are derived below, to further analyze

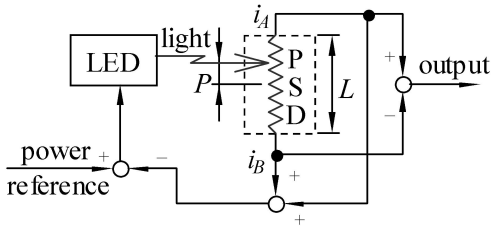

Fig. 5 Signal conditioning in optical pick-ups

the mechanical sensitivity. Inertia of the outer ring of the flexible disc is

$$J = \frac{1}{32}\rho\pi b_R(d_1^4 - d_2^4)\,, \tag{4}$$

where ρ is material specific density, b_R is thickness of the ring, and d_1 and d_2 are outer and inner diameters of the ring, respectively. Stiffness of the flexible bars is expressed by

$$k = \frac{2Na^3 b_S E d_{S1}^2}{(d_{S1} - d_{S2})^3}\,. \tag{5}$$

Here N is number of the flexible bars, a and b_S are width and thickness of one of the flexible bars, respectively, E is Young's modulus, and d_{S1} and d_{S2} are an inner diameter of the outer ring and an outer diameter of the inner ring of the flexible disc, respectively.

An important result is obtained when thickness of the outer ring and thickness of the flexible bars are equal ($b_R = b_S$). In this case introducing eqs. (4) and (5) into eq. (3) gives a formula for mechanical sensitivity, in which the thickness is canceled. This means that the mechanical sensitivity of the sensor is independent of thickness of the flexible disc, if the disc is of an even thickness. This is an important feature of the proposed sensor, that can be profitably used in the production process, since it enables a wider selection of the technology to produce the flexible disc.

3. 2 Optical Sensitivity

Optical sensitivity of the sensor is defined as a ratio of the radial displacement of the slits crossing sections to the angular displacement ϕ. Geometrical parameters of the slits are shown in **Fig. 6**. Here r_0 is radial distance from the center of the flexible disc to the slits crossing sections in the steady state with no acceleration applied, r is radial distance from the center of the flexible disc to the slits crossing sections at applied acceleration in the steady state (dashed line represents a displaced slit), and α is an inclination angle between the slits of both discs.

A radial displacement of the slits crossing section is denoted as $(r - r_0)$, and the optical sensitivity of the sensor S_O is defined by eq. (6)

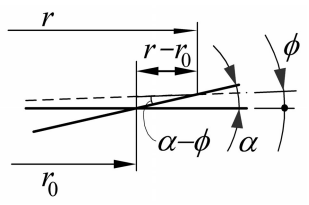

Fig. 6 Geometrical parameters of the crossing slits

$$S_O = \frac{(r - r_0)}{\phi} \approx \frac{r_0}{\tan\alpha}\,. \tag{6}$$

Note that the approximate expression of the optical sensitivity $r_0/\tan\alpha$ is derived from a relation $r_0\phi \approx (r - r_0)\tan(\alpha - \phi)$. This approximation can be used when the displacement angle ϕ is small, comparing to the size of the slits crossing angle α. An exact expression of the optical sensitivity with the straight slits in Fig. 6 is denoted by a differential equation

$$S_O = \frac{dr}{d\phi} = \frac{r}{\tan(\alpha - \phi)}\,. \tag{7}$$

This equation indicates that the optical sensitivity of the straight slits is a function of the radius to the slits crossing sections and of the angular displacement ϕ. This means that the sensor's output is nonlinear in this case. Linearity can be improved by suitable modification of the slits' shape. A pattern of the slits to produce constant optical sensitivity is derived in the next section.

4. Pattern of Slits for Linear Output

As it was indicated in eq. (7), optical sensitivity of the straight slits produces nonlinear output. A condition to obtain linear characteristics of the sensor is provided by constant optical sensitivity: the sensitivity is independent of the angular displacement ϕ.

From a condition

$$S_O = \frac{dr}{d\phi} = \text{const.} \tag{8}$$

we can get a needed pattern of the slits by integration. The result is

$$r = r_0 + S_O\phi\,. \tag{9}$$

This explains that the inclined slits must be shaped into Archimedes' spirals with constant gradient which is equal to the optical sensitivity. The slits with such shape satisfy the condition for constant optical sensitivity S_O and assure linearity of the sensor's output.

Slits of the discs are mostly fabricated by photo etching process. Therefore, it is relatively simple to practically produce the slits with a shape of Archimedes' spiral.

5. Analysis of Effect of Eccentricity

When both discs of the sensor are mounted on a shaft, two types of eccentricity can appear. One is an eccentricity of the center of the shaft, relative to the rotation center, and the other is an eccentricity of the centers of the two discs, relative to each other. The effect on the output of the sensor is analyzed in the following discussion.

The eccentricity of the shaft is caused by misalignment of the rotation center relative to the center of the shaft. The eccentricity produces a harmonic error in the output

of the sensor when the shaft rotates. A period of the error is equal to one turn of the shaft. This error can be compensated by addition of two signals from the pick-ups, which are placed apart at 180° angular positions.

The eccentricity of the discs (centers of the slits are miss-aligned) has more complex influence on the output of the sensor. The relations are analyzed in the next section by comparison of the outputs at ideal conditions, that is at no eccentricity, and at some eccentricity.

5. 1 Output of the Sensor Without Eccentricity

At the ideal conditions, when both centers of the discs are aligned, there is no eccentricity, and only one pick-up on one side of the discs is sufficient. To obtain equations that can be afterwards used for comparison to the results with an eccentricity we assume, that there are initially two pick-ups built in the sensor. Output of the sensor U is described by eq. (10) (refer to **Fig. 7**).

$$U = r_1 + r_2 - 2r_0 = 2S_O\phi \tag{10}$$

Here r_1 and r_2 are radial distances from the discs' center to the crossing sections on both opposite sides, respectively. They are defined by eq. (9), and here introduced into eq. (10), so that we have the last expression in eq. (10). Output of the sensor is in this case proportional to the angular displacement ϕ, as we expected.

5. 2 Output of the Sensor With Discs' Eccentricity

A situation with miss-aligned centers of the discs is shown in **Fig. 8**. Centers of the slits are dislocated for orthogonal eccentricity distances e_x and e_y in planar Cartesian coordinate system. Subscripts 1 and 2 are added to the parameters of opposite sides of the discs, respectively.

To graphically analyze influences of the eccentricity on the sensor's output, the slits from both sides of the discs are plotted together on one side, and aligned so that the curved slits of both sides overlap, as it is shown in **Fig. 9**.

By inspection of Fig. 9, the following can be concluded:

- There is a difference between the initial distances r_{01}, r_{02}, and the distance r_0 because of the eccentricity displacement e_x.
- The displacement e_y causes an additional difference in the initial distances r_{01} and r_{02}, and produces a difference in the sum of the two distances comparing to the conditions without eccentricity ($r_{01} + r_{02} \neq 2r_0$). This difference appears because of an equal displacement e_y but into different directions of the curved slits: the initial inclination angle of the curved slit in the so obtained crossing sections differs. This causes r_{01} to shrink more than r_{02} prolongs. In this way an initial offset in the output of the sensor appears. The offset is then compensated by electrical signal conditioning.
- The displacement angle ϕ produces a radial displacement of the slits crossing points from the initial radii r_{01} and r_{02} to the new radii r_1 and r_2, respectively. Because of the difference in inclination angles of the curved slits at the crossing points and because of the different engagement angles φ_1 and φ_2 on Archimedes' spirals on respective sides (see Fig. 9), it can be shown that the output of the sensor deviates by the size of eccentricity distances e_x and e_y.

Conclusion: An eccentricity is significantly reduced, though not ideally compensated by the two pick-ups, when the curved slits are used.

A way to perform qualitative analysis of the uncompensated error is to derive mathematical equations, and to solve them. Mathematical analysis of the error can be found in Appendix. A numerical example in the appendix shows that practically the uncompensated error is very small because of a small displacement angle ϕ and because of a relatively small eccentricity comparing to the size of the radius of the slits.

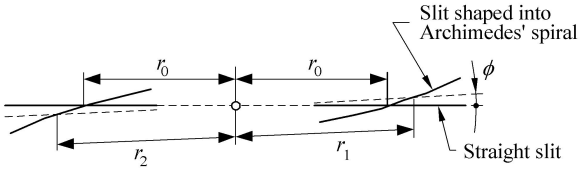

Fig. 7 Slits' crossing sections without eccentricity

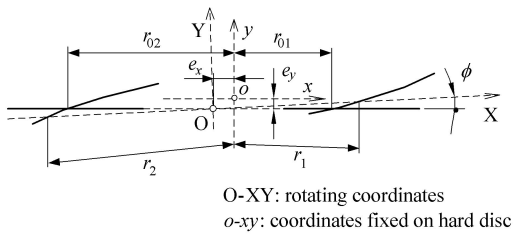

Fig. 8 Crossing of the slits with miss-aligned centers

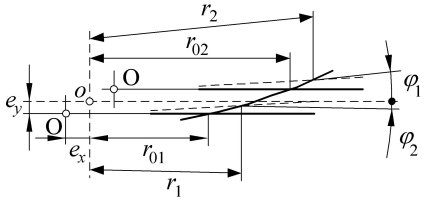

Fig. 9 Both sides of discs plotted with overlapping curved slits

6. Experimental Results

We built two kinds of prototypes of the proposed sensor. One is a small size and low sensitivity type [6], which is to be used in servomotors, and the other one is a large size and high sensitivity type [7], which is to be used on low speed shafts, for example in robot joints. Slits of a low sensitivity device are formed as Archimedes' spirals, while the Archimedes' spiral of the slits of a high sensitivity device is equivalent to the straight line, due to a high gradient of the spiral. Main characteristics of the prototype devices are shown in **Table 1**. Rated accelerations of the prototypes were selected so that the sensitivities are satisfactory for our experimental equipment, while the stress in the flexible bars at three-times of the rated acceleration does not cause any non-elastic deformation.

A response of the high sensitivity prototype sensor is depicted by curve 'Sensed' in **Fig. 10**. The sensor was coupled to the output shaft of the experimental equipment, which is composed of a DC brushless servomotor (100 W), a strain wave gearing (reduction ratio 1/100), and inertia load. A fourth order Butterworth low-pass filter with a cut-off frequency of 600 rad/s was used to cut-off the natural vibration of the sensor.

Table 1 Characteristics of prototype sensors

Performance	Symbol	Type of device	
		Low sensitivity	High sensitivity
Natural frequency	ω_n	4200 rad/s	2200 rad/s
Slits radius	r_0	16 mm	36 mm
Optical sensitivity	S_O	107 mm/rad	1.53 m/rad
Rated acceleration		$\pm 3 \times 10^4$ rad/s^2	± 200 rad/s^2

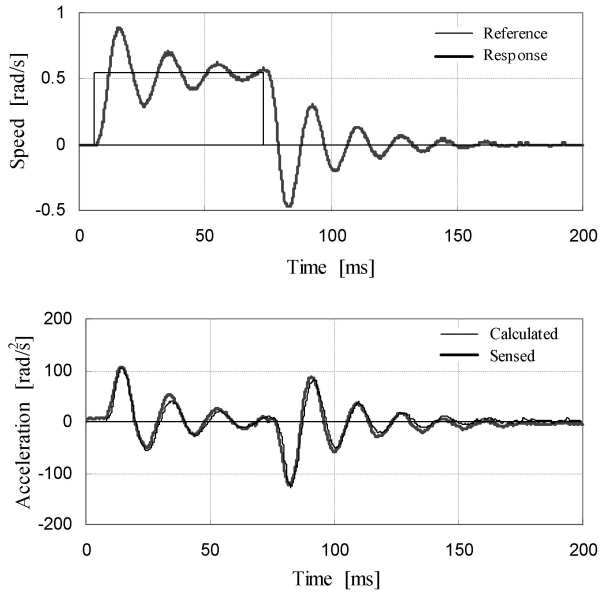

Fig. 10 Response of prototype sensor

The shaft speed and the calculated acceleration are shown in the same figure. The calculated acceleration was obtained as a time derivative of the position, which was measured by a 360,000 pulse per revolution incremental encoder. A second order low-pass filter with a cut-off frequency of 600 rad/s was used to reduce high frequency noise. The calculated and the sensed accelerations are in good accordance; except some positive offset error at the beginning of the experiment and some negative offset error at the end of the experiment. The errors are caused by mechanical inaccuracies of the prototype, which are being studied to be reduced in the future designs.

7. Conclusion

A novel type of angular acceleration sensor has been proposed. In this paper we presented some significant features of the sensor. A structure of the device was explained, and equations for the sensitivity of the sensor were derived. A section of Archimedes' spiral was proposed to be used for the slits' pattern, to improve linearity of the sensor's output.

Influence of the assembly eccentricities on the output of the sensor was studied. It was shown that the eccentricity can be satisfactory compensated by placing two identical optical pick-ups diametrically on opposite sides of the discs. An experimental result with a high sensitivity prototype device shows good accordance of the calculated and the sensed accelerations.

Advantage of the proposed device is non-contact sensing of angular acceleration, which is realized by two discs with slits on the peripheries and by two optical pick-ups. This configuration also enables speed independent sensing and unlimited rotational range of the device. The sensor has sufficient sensitivity for most applications and can be directly mounted on rotating shaft. Slits on the discs are similar to those of an incremental encoder, therefore, the same production technology as for the pulse encoders can be used.

Mechanical sensitivity of the sensor is in inverse proportion to the square of the natural frequency of the sensor: the natural frequency of the sensor must be low to reach high mechanical sensitivity. A lack of mechanical sensitivity, which can arise from the specified frequency characteristic of the sensor, can be supplemented by sufficient optical sensitivity.

References

1) Y. Konno and Y. Hori: Instantaneous Speed Observer with Improved Disturbance Rejection Performance Based on Higher Order Dynamics (in Japanese), T. IEE Japan, **112**–**D**–6, 539/544 (1993)
2) H. Kamei and Y. Hori: High Performance Control of Servo-Motor with Low Accuracy Encoder – Instantaneous Speed Observer and Adaptive Estimation of Inertia – (in Japanese), Technical Bulletin IEE Japan, **IIC**–**93**–15, 66/78 (1993)
3) A. Shimada: Analysis of Estimation Error on Observer for Disturbance and Velocity (in Japanese), T. IEE Japan, **113**–**D**–7, 874/882 (1993)
4) J. C. Boomgaarden: Design of Induction Angular Acceleration Sensors for Dynamic Response, Linearity, and Minimum Harmonic Noise, Ph.D. Thesis, University of Wisconsin–Madison (1993)
5) N. Furukawa and K. Ohnishi: A Structure of Angular Acceleration Sensor Using Silicon Cantilever Beam, Proc. IECON'92, 1524/1529 (1992)
6) I. Godler, A. Akahane, K. Ohnishi and T. Yamashita: Rotary Acceleration Sensor for Robust Control, Proc. SICE'93 International Session, 1317/1322 (1993)
7) I. Godler, A. Akahane, M. Kaneko and T. Yamashita: Angular Acceleration Sensor for Robot Joints, Proc. 11th RSJ Symp., 963/966 (1993)
8) M. Idesawa and H. D. Ding: RHPSD and Its Multi-Resolution Image Position Sensing Characteristics, T. SICE, **29**–2, 152/158 (1993)

Appendix A.

A mathematical analysis of the effect of the slits' eccentricity to the sensor's output is given in the appendix. The derived equations relate to the variables shown in Figs. 8 and 9. The objective here is to derive mathematical expressions for the radial distances r_1 and r_2 at arbitrary eccentricity conditions, which are represented by orthogonal eccentricity distances e_x and e_y.

To analyze the output of the sensor with slits' eccentricity, a coordinates transformation of the slits crossing sections from the coordinate system *o–xy* into the coordinate system O–XY is needed. Coordinates of the centers of the slits crossing sections as a function of the angle φ_i in the *o–xy* coordinate system are, referring to eq. (8)

$$\left.\begin{aligned} x_i &= r_{0i} + S_O \cos\varphi_i \\ y_i &= r_{0i} + S_O \sin\varphi_i \end{aligned}\right\}, \quad i = 1, 2\,. \tag{A. 1}$$

Here angles φ_i are the engagement angles on Archimedes' spiral. Note that if the eccentricity exists, angles φ_i are not equal to the slits displacement angle ϕ. The coordinates x_i, and y_i are transformed into the O–XY coordinate system first by translation and then by rotation:

$$\left\{\begin{matrix} X \\ Y \end{matrix}\right\} = \begin{bmatrix} \cos\phi & -\sin\phi \\ \sin\phi & \cos\phi \end{bmatrix} \left\{\begin{matrix} x + e_y \\ y + e_y \end{matrix}\right\}. \tag{A. 2}$$

From this relation, written for the slits crossing sections of both sides and with eq. (A.1) introduced into the consideration, a system of four nonlinear equations is obtained.

$$\begin{aligned} r_1 &= (r_0 + S_O\varphi_1)(\mathrm{c}\varphi_1\mathrm{c}\phi + \mathrm{s}\varphi_1\mathrm{s}\phi) + e_x\mathrm{c}\phi + e_y\mathrm{s}\phi \\ -r_2 &= -(r_0 + S_O\varphi_2)(\mathrm{c}\varphi_2\mathrm{c}\phi + \mathrm{s}\varphi_2\mathrm{s}\phi) + e_x\mathrm{c}\phi + e_y\mathrm{s}\phi \\ 0 &= (r_0 + S_O\varphi_1)(-\mathrm{c}\varphi_1\mathrm{s}\phi + \mathrm{s}\varphi_1\mathrm{c}\phi) - e_x\mathrm{s}\phi + e_y\mathrm{c}\phi \\ 0 &= -(r_0 + S_O\varphi_2)(-\mathrm{c}\varphi_2\mathrm{s}\phi + \mathrm{s}\varphi_2\mathrm{c}\phi) - e_x\mathrm{s}\phi + e_y\mathrm{c}\phi \end{aligned} \tag{A. 3}$$

The abbreviations c for cos and s for sin are used to save space. Output of the sensor can be derived from the first two equations of the above system of equations.

$$\begin{aligned} U = r_1 + r_2 - 2r_0 &= (r_0 + S_O\varphi_1)\cos(\varphi_1 - \phi) \\ &\quad + (r_0 + S_O\varphi_2)\cos(\varphi_2 - \phi) - 2r_0 \end{aligned} \tag{A. 4}$$

Here it appears that the eccentricities e_x and e_y have no influence on the output: directly they have no influence, but indirectly by the angles φ_1 and φ_2 they influence the output. To prove this, the angles φ_1 and φ_2 are to be derived from the last two equations of eqs. (A.3) and then introduced into eq. (A.4). This is a difficult task to be done analytically. In the following numerical example the angles φ_1 and φ_2 are found numerically.

A. 1 Numerical Example

Let us consider to have an angular acceleration sensor with the following properties:

$r_0 = 16\mathrm{mm}$,
$S_O = 107\mathrm{mm/rad}$,
$\phi = 6.25 \times 10^{-4}\mathrm{rad}$ ($\approx 2.15\mathrm{arc\ min}$).

In this case the output of the sensor without eccentricity is $U = 2S_O\phi = 133.73\,\mu\mathrm{m}$. Output with eccentricity of $e_x = e_y = 10\,\mu\mathrm{m}$ and one pick-up has more than $10\,\mu\mathrm{m}$ of error amplitude, while the output with two pick-ups is $U = 133.1923\,\mu\mathrm{m}$.

The error in the output caused by the eccentricity of the discs is therefore compensated to $-0.558\,\mu\mathrm{m}$ (0.42%). This shows that in practical conditions when both the eccentricity and the displacement angle ϕ are small, influence of the eccentricity is significantly reduced by the two optical pick-ups, here from more than $10\,\mu\mathrm{m}$ to less than $0.6\,\mu\mathrm{m}$. This consideration is mathematically proved in the next section.

A. 2 Linearization of Equations for the Sensor's Output

As we showed by the above numerical example, in practical conditions the displacement angle is small, therefore the following two steps of linearization can be applied:

$$\begin{aligned} &\text{first} && \cos\varphi_1 = \cos\varphi_2 = \cos\phi = 1, \\ & && \sin\varphi_1 = \varphi_1, \sin\varphi_2 = \varphi_2, \sin\phi = \phi, \quad \text{(A. 5)} \\ &\text{second} && \varphi_1^2 = \varphi_2^2 = \varphi_1\phi = \varphi_2\phi = 0. \end{aligned}$$

In this way the system of eqs. (A.3) is reduced to a system of linear equations

$$\begin{aligned} r_1 &= r_0 + S_O\varphi_1 + e_x + e_y\phi \\ -r_2 &= -r_0 - S_O\varphi_2 + e_x + e_y\phi \\ 0 &= r_0\varphi_1 - r_0\phi - e_x\phi + e_y \\ 0 &= -r_0\varphi_2 + r_0\phi - e_x\phi + e_y \end{aligned} \quad \text{(A. 6)}$$

From this system of equations we can see that the sensor's output U is

$$U = S_O(\varphi_1 + \varphi_2)\,, \quad \text{(A. 7)}$$

and the angles φ_1 and φ_2 are

$$\begin{aligned} \varphi_1 &= \frac{r_0\phi + e_x\phi - e_y}{r_0}, \\ \varphi_2 &= \frac{r_0\phi - e_x\phi + e_y}{r_0}. \end{aligned} \quad \text{(A. 8)}$$

Introducing eqs. (A.8) into eq. (A.7) shows that the output of the sensor is

$$U = 2S_O\phi\,. \quad \text{(A. 9)}$$

This proves that the influence of the discs' eccentricity is sufficiently compensated when the displacement angle ϕ is small, comparing to the size of the slits crossing angle α.

Ivan Godler (Member)

He received the B. E. degree from Faculty of Mechanical Engineering, University of Ljubljana, Slovenia in 1986, and the M. E. and Dr. E. degrees in 1991 and 1995 from Kyushu Institute of Technology, Kitakyushu, Japan, both in control engineering. He is now an assocoate professor at the University of Kitakyushu, Department of Information and Media Sciences. His research interests include motion control, vibration suppresion control, and sensing.

Akira Akahane

He received the B. S. degree in 1972 from Faculty of Science and Technology, Science University of Tokyo, Japan in physics. He is now employed by Harmonic Drive Systems, Inc,. Nagano, Japan. His activities are in the fields of servomotor control, vibration suppression control, optics, and position and force sensing.

Toshiki Maruyama

He received the B. E. and M. E. degrees in 1978 and 1981 respectively from Faculty of Engineering, Shinshu University, Nagano, Japan, both in electrical engineering. He is now employed by Harmonic Drive Systems, Inc,. Nagano, Japan. He works on the research and development of AC servomotors and new electromagnetic actuators.

Tadashi Yamashita (Member)

He received the B. S. degree from Kyushu Institute of Technology, Kitakyushu, Japan, and the M. E. and Dr. E. degrees in 1963 and 1966 respectively from the University of Tokyo, Japan, all in mechanical engineering. He is now a professor of control engineering at Kyushu Institute of Technology, Kitakyushu, Japan. His research interests include robust motion control, robust stability theory, fuzzy control, computer assisted telerobotic systems, and dynamics and simulation of human walking.

Reprinted from Trans. of the SICE, Vol.31, No.8, 982/990 (1995)